Journal of Molecular Graphics and Modelling 52 (2014) 11–19

Contents lists available at ScienceDirect

Journal of Molecular Graphics and Modelling

journal homepage: www.elsevier.com/locate/JMGM

Homology modelling, docking, pharmacophore and site directed mutagenesis analysis to identify the critical amino acid residue of PknI from *Mycobacterium tuberculosis*

Srinivasan Kandasamy[a], Sameer Hassan[b], Radha Gopalaswamy[a], Sujatha Narayanan[a,*]

[a] Department of Immunology, National Institute for Research in Tuberculosis (NIRT) (ICMR), Chetput, Chennai 600 031, Tamilnadu, India
[b] Department of Biomedical Informatics, National Institute for Research in Tuberculosis (NIRT) (ICMR), Chetput, Chennai 600 031, Tamilnadu, India

ARTICLE INFO

Article history:
Accepted 28 May 2014
Available online 4 June 2014

Keywords:
Protein kinases
Homology modelling
Site directed mutagenesis
Substrate
Docking
Pharmacophore analysis

ABSTRACT

Tuberculosis is caused by *Mycobacterium tuberculosis*, an intracellular pathogen. PknI is one of the 11 functional Serine/Threonine Protein Kinases which is predicted to regulate the cell division of *M. tuberculosis*. In order to find newer drugs and vaccine we need to understand the pathogenesis of the disease. We have used the bioinformatics approach to identify the functionally active residues of PknI and to confirm the same with wet lab experiments. In the current study, we have created homology model for PknI and have done comparative structural analysis of PknI with other kinases. Molecular docking studies were done with a library of kinase inhibitors and T95 was found as the potent inhibitor for PknI. Based on structure based pharmacophore analysis of kinase substrate complexes, Lys 41 along with Asp90, Val92 and Asp96 were identified as functionally important residues. Further, we used site directed mutagenesis technique to mutate Lys 41 to Met resulting in defective cell division of *Mycobacterium smegmatis* mc^2. Overall, the proposed model together with its binding features gained from pharmacophore docking studies helped in identifying ligand inhibitor specific to PknI which was confirmed by laboratory experiments.

1. Introduction

Tuberculosis (TB) caused by *Mycobacterium tuberculosis* (*M. tuberculosis*) *is* one among the devastating disease that kills 1.4 million people every year [1]. In spite of global awareness for drug resistant TB, Multi drug resistant (MDR) and extensively drug resistant (XDR) TB continue to emerge in high HIV prevalence setting, and the mortality rate in HIV co-infected patients remains high. *Mycobacterium bovis* Bacillus Calmette Guerin (BCG), the currently available vaccine, can be used only for severe forms of childhood TB, but its efficacy against pulmonary TB in adults remains controversial [2]. The success of *M. tuberculosis* results from its remarkable capacity to survive within the infected host, where it can persist in a non-replicating state for several decades. Protein phosphorylation is the principal mechanism involved in translating extracellular signals into cellular responses and this process is carried out by specific protein kinases [3].

M. tuberculosis genome consists of 11 Serine Threonine Protein Kinases (STPKs) (PknA–PknL). Among the 11 STPKs, nine are transmembrane receptors with kinase domain located within the cell (PknA, PknB, PknD, PknE, PknF, PknH, PknI, PknJ and PknL) and two kinases are soluble proteins (PknG and PknK) [4,5]. These STPKs have been suggested to play significant roles by influencing diverse signalling pathways depends upon the bacterial environmental conditions. PknA, PknB and PknF was functionally characterized and found to play a role in cell division [6–10]. Besides cell division PknF also plays a role in biofilm formation and glucose transport [10,11]. Five of the STPKs namely PknI, PknE, PknG, PknH, and PknK are reported to support intracellular survival [12–16]. PknL plays a role in starvation response [17].

In analogue with other *M. tuberculosis* STPKs, PknI also possesses N-terminal cytosolic domain and C-terminal extracellular domain. The C-terminal domain of STPKs is thought to sense environmental changes, which are communicated to the internal milieu through the N-terminal domain constituting the active site of the kinase [18]. Based on the sequence analysis of the kinase domain of *M. tuberculosis* STPKs, PknI is positioned in the same clade as that of PknF and PknJ [19]. These observations provide some insights into

* Corresponding author at: Scientist 'G', Department of Immunology, National Institute for Research in Tuberculosis (NIRT) (ICMR), Chetput, Chennai 600 031, Tamilnadu, India. Tel.: +91 44 28369627; fax: +91 44 2836 2528; mobile: +91 9444057490.
E-mail address: sujatha.sujatha36@gmail.com (S. Narayanan).

http://dx.doi.org/10.1016/j.jmgm.2014.05.011
1093-3263/

the evolution of PknI. In the *M. tuberculosis* genome, PknI, is flanked by the DacB2, FtsY and Ffh genes involved in cell division and protein secretion, indicating a possible role for PknI in one of these processes [4]. The sequence comparison analysis of PknI with other prokaryotic STPKs revealed its close homology to Stk1 from *Streptococcus agalactiae*, which was shown to play a role in the virulence and cell segregation of the organism. The genes for PknA, PknB and PknI, are located within the same operons that are known to be involved in cell division in *Escherichia coli* and *Bacillus subtilis*; thus it has been suggested that PknI may be involved in the regulation of bacterial cell division [4]. Previously, we have reported that PknI has a functionally active kinase activity and showed manganese dependent auto-phosphorylation at serine and threonine residues [20].

We found that the, PknI over-expression, leads to growth retardation and cell elongation in non pathogenic *Mycobacterium smegmatis* mc^2 (unpublished data). The PknI knockout strain of *M. tuberculosis* regulates the growth under stress conditions like acidic pH and low oxygen availability. PknI plays a role in sensing the macrophages host environment and translating it to slow the growth of *M. tuberculosis* within the infected host. Moreover, PknI Knockout strain of *M. tuberculosis* showed hyper-virulence phenotype in severe combined immunodeficiency (SCID) mice when compared to wild type strain [12]. Overall, we demonstrated that the PknI has a role in cell division and virulence of *M. tuberculosis*.

PknI has two unique distinguishing features when compared with other kinases. Firstly, though the PknI has a transmembrane domain surprisingly it's localized predominantly in the cytosol. Secondly, the expression pattern of PknI differs from that of other kinases, as exemplified by comparison with PknA and PknB: PknI decreases significantly over the course of infection of macrophages, while expression of PknA and PknB increases [21].

For the current study, we have used computational approach to predict the three dimensional structure of PknI. Homology modelling approach produces valid structural models for protein sequences with available related templates (having > 30 percentage amino acid sequence identity) [22]. Comparative study of these models with the known protein structures in Protein Data Bank (PDB) will help in understanding the similarities that may also facilitate inferring biochemical and biological functions [23].

In the present study, we have developed three dimensional model for PknI protein in order to predict the evolutionarily conserved and functionally important amino acids which are crucial for its kinase activity. This was further proved by using site directed mutagenesis studies. A pharmacophore model was developed by using both structure and ligand based methods. The best model was used to screen a library of compounds using GOLD docking methodology.

2. Materials and methods

2.1. Sequence alignment, secondary structure prediction

Protein sequence of *M. tuberculosis* Ser/Thr protein kinase, PknI (Swissprot: P65730) was used. ClustalW [24] and Align Multiple Sequences of Discovery Studio (DS) v 2.0 enabled the alignment of multiple sequences. Jpred: A Consensus Secondary Structure Prediction Server was used to predict secondary structure elements of PknI. Insertions were manually adjusted to preserve secondary structural features in PknI.

2.2. Template selection and homology modelling

The amino acid sequence of PknI protein was subjected to PSI-BLAST [25] and Phyre2 [26] to identify the most suitable crystal structure in PDB [27] database as template for modelling PknI. The best template was selected based on sequence identity, domain coverage, resolution, E-value and bound with cognate ligand. Based on sequence search and fold recognition, 1O6Y, PknB kinase from *M. tuberculosis*, was selected as template (32% identity and 3e−25 *E*-value). We used the homology modelling procedure such as MODELLER [28] which works well in the range of 30–40% identity between sequences. MODELER is able to simultaneously incorporate structural data from one or more reference proteins. Structural features in the reference proteins are used to derive spatial restraints which, in turn, are used to generate model protein structures using conjugate gradient and simulated annealing optimization procedures. Homology modelling of PknI was done using MODELLER, Discovery Studio v 2.0. We used PROCHECK [29] to check the geometry and stereochemical quality of our predicted structures and environment profile using VERIFY-3D [30] graph. Models were developed using different alignments and the best model was selected for further analysis. The final model was also superimposed with the template structure using PBDefold [31] for calculating the backbone RMSD.

2.3. Docking of substrate and drugs

Gold (Genetic Optimization for Ligand Docking, version 5.2) was used to dock the substrate and drugs in the active site to obtain the conformation and orientation. GOLD uses a genetic algorithm methodology for protein ligand docking that allows full ligand and partial protein flexibility. The modelled PknI structure was used for docking process, hydrogen atoms were added. The ATP and drug molecules were corrected using the LigPrep and Auto Edit Ligand option in Schrodinger and GOLD program respectively. The binding site of ATP was mapped based on known kinases complexes present in PDB and was provided an input for GOLD calculation. Default genetic algorithm (GA) settings that ensure 100% search efficiency were used for docking. An early termination of the number of GA runs was allowed when the RMSDs of the top three GA solutions were within 1.5 Å. The best pose of the docked ligand was selected based on CHEMPLP score.

2.4. Site directed mutagenesis of PknI

The site directed mutagenesis was done as described previously [11]. Briefly, PCR amplifications were done using Taq DNA polymerase (Roche) and genomic DNA of *M. tuberculosis* H37Rv as the template. Restriction enzyme recognition sites were added to the primers to facilitate in frame and directional cloning as indicated. The PknI coding region was PCR amplified using the oligo 1 and 2 (Table 1), and cloned into the BamHI and EcoRV site of pSD26 containing an acetamidase promoter and C-terminal His tag to create pRG5 (Table 1). The *PknI* gene was cloned without its stop codon in frame to a His tag and a stop codon was introduced immediately after the tag. The coding region of *PknI* was amplified using the primers, oligo 3 and 4 as primers and cloned into the pMV261 which carried an *hsp60* promoter. Replacement of the ATP-binding domain lysine (K) at position 41 to methionine (M) was performed using a Quik-Change site directed mutagenesis kit (Stratagene) following the supplier's instructions. The primers used for creating lysine to methionine mutation were Oligo 5 and 6 (Table 1). The sequences of all the constructs were confirmed by automated sequencer (Applied Biosystem Genetic Analyzer, model 3100).

2.5. Overexpression of PknI gene in M. smegmatis mc^2

Plasmids pSD26, pRG5 and pRG5–K41M were introduced into *M. smegmatis* by electroporation. Mycobacterial cells were lysed

Table 1
List of primers, plasmids and strains used in this study.

Strain/primers/plasmid	Description	Source
pSD26	*E. coli – Mycobacterium* shuttle vector carrying acetamidase promoter; Hyg^r	[49]
pMV261	*E. coli – Mycobacterium* shuttle vector carrying *hsp60* promoter; Kan^r	[50]
pRG5	pSD26 harbouring 1758 bp *PknI* of *M. tuberculosis*	This study
pRG5–K41M	pSD26 harbouring 1758 bp *PknI* of *M. tuberculosis* bearing a K to M mutation at position 41	This study
Strains		
Mc^{2}4806	*M. smegmatis* bearing pSD26	This study
Mc^{2}4807	*M. smegmatis* bearing pRG5 overexpressing *PknI*	This study
Mc^{2}4808	*M. smegmatis* bearing pRG5-K41M overexpressing	This study
Primers		
Oligo 1	5′-GGAAGATCTTCCATGGCGTTGGCCAGC-3′	This study
Oligo 2	5′-GATATCGCGACCGGGCCCCGGCG-3′	This study
Oligo 3	5′-GAATTCATGGCGTTGGCCAGCGGCGT-3′	This study
Oligo 4	5′-CCCAAGCTTGGGTCAGCGACCGGGCCCCGGCG-3′	This study
Oligo 5	5′-CAGGCGCTGAtGGTGCTTTC-3′	This study
Oligo 6	5′-GAAAGCACCaTCAGCGCCTG-3′	This study

following induction and analyzed by Western blot against the His-tag of the protein as described previously [11].

Fresh grown log-phase cultures of mc^{2}4806, mc^{2}4807 and mc^{2}4808 were diluted in fresh LB with 0.05 (vol/vol) Tween80 to an initial OD_{600} of 0.05. One set of cultures was induced with 0.2% of acetamide and aliquots of 1 ml were removed from cultures for OD_{600} readings at various time points to monitor growth. The growth kinetics was performed with triplicate samples. Cells were grown in the presence or absence of acetamide for 15 h and then plated with or without acetamide to study the differences in viability.

2.6. Structure based pharmacophore analysis

The structure based pharmacophore analysis was performed using LigandScout [32] to identify the interaction of critical residues between the protein and ligand. This method is becoming important because of the huge number of X-ray crystal structure complexes deposited in PDB database. It is earlier reported that, the protein structure information is a good source for structure based pharmacophore and can be used as screening before docking studies [33,34]. LigandScout was used for the construction and visualization of pharmacophore features derived from the three dimensional coordinates of the protein structures. Interactions such as hydrogen bond, charge transfer, hydrophobic regions from the PDB files are extracted using the software. Hydrogen bond acceptor/hydrogen bond donor is considered on the protein structure within the limits of geometric constraints. Excluded volumes are defined as inaccessible areas of protein side chains for any potential ligand.

3. Results and discussion

The "eukaryotic-like" receptor Ser/Thr protein kinases (STPKs) are candidates for the sensors that mediate environmental adaptations of *M. tuberculosis*. PknI is one among 11 protein kinases encoded by mycobacterial genome. Crystal structures of PknB [35], PknD [36], PknE [37], PknH [38] and PknG [39] have been reported. PknI protein has a kinase domain (12–240) at the N-terminal region and a transmembrane helix between 350 and 370 amino acids long (Fig. 1).

The basic idea of homology modelling is to develop a three dimensional structure of a protein making use of the collected body of knowledge from the previously resolved homologous protein crystal structures. Several crystal structures for the kinase domain from *M. tuberculosis*, human and other organisms have been reported by different research groups [40,41]. Since the structure for 585 residues long PknI having a kinase domain at the N-terminal is not known, and the enzyme being a rational target for structure based molecular design, a homology model was developed.

3.1. Comparative analysis of 11 protein kinases of M. tuberculosis

The protein kinase domain of 11 STPKs of *M. tuberculosis* was aligned using Align Multiple Sequence module of Discovery Studio. Since the C-terminal of these kinase proteins varied, they were removed from the sequence for attaining an accurate alignment. Based on the alignment, the kinase domains are moderately conserved in the N-terminus than in the C-terminus. The nucleotide binding site and the DFG motif are highly conserved. Though the activation loop is highly variable among the kinase proteins with highly conserved threonine residue (auto-phosphorylation sites), is totally absent in PknI protein. The mode of substrate binding with PknI is questionable.

3.2. Molecular modelling of PknI and docking of ATP

The crystal structure of PknB (1O6Y) [42] in tight binding conformation served as the template, which should logically be closer to the conformation adopted by the enzyme in a physiological environment. Selecting template structures in complex with cognate ligands are important as the conformation of bound structures have a critical role to play in docking or virtual screening [43]. Secondary structure and fold recognition analysis, supported PknB (PDB code: 1O6Y) as ideal template for homology modelling of PknI kinase domain (Residue: 12–251). We have used MODELLER program of DS v 2.0 to produce a homology based model of kinase domain of PknI. The N-terminal kinase domain of PknI was selected because it showed high sequence identity to the kinase domain of PknB (Fig. 2).

While 30% sequence identity is generally considered to be the threshold limit for accurate homology modelling and as MODELLER works well within the range 30–40% sequence identity [44], homology modelling of kinase domain of PknI based on PknB crystal structure would presumably yield a reliable structure. Of the 10 different models generated, the one showing the lowest energy,

Fig. 1. Domain organization of PknI: PknI having the kinase domain (grey) and transmembrane helix (green). (For interpretation of the references to color in this figure legend, the reader is referred to the web version of this article.)

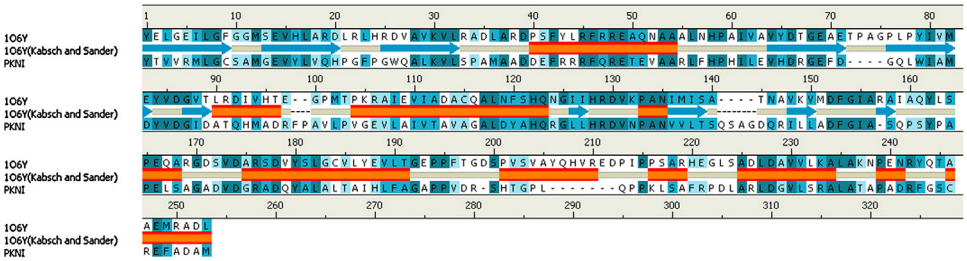

Fig. 2. Sequence alignment of PknI and PknB (1O6Y): It was performed using Align Multiple Sequences protocol in Discovery Studio v2.0. Identical or conserved amino acids are shaded. Catalytic residues are indicated by asterisks. The secondary structure elements such as helices and strands are shown as red cylinder and blue arrow respectively. (For interpretation of the references to color in this figure legend, the reader is referred to the web version of this article.)

restraint violations, and having the least number of main chain and side chain bad conformations was selected.

Based on the alignment produced using DS, all residues from 12 to 251 of kinase domain were modelled. Inspection of the final model and the underlying alignment between PknI and PknB, which served as the base for the modelling, indicates that the insertions between 93 and 96, between 136 and 141 occurred in the loop regions where as of the two deletions 71–72 and 199–200 in PknI occurred in the loop region and in α-helix respectively. This indicates a reliable alignment and is a prerequisite for homology modelling of good quality. The structural framework of the active site of PknI that is dictated by the fold and residues of the catalytic domain which exhibits higher sequence identity than the rest of the protein, further supports the predictive value of our model. The topology of PknI fold is shown in supplementary Fig. 1. Thus, the model indicates that PknI possess an active site similar to that of PknB and other kinase domains, which contains the catalytic residues Lys7, Gly8, Cys9, Ser10, Ala11, Met12, Gly13, Glu14, Val15, Lys 41, Asp126.

Supplementary Fig. 1 related to this article can be found, in the online version, at http://dx.doi.org/10.1016/j.jmgm.2014.05.011.

The best model with lowest PDF value obtained for PknI kinase domain (12–251) is shown in (Fig. 3A). The quality of this model was evaluated using PROCHECK. The initial model which showed 90.6% residues in the most favoured region (and 1 residue in the disallowed region) of Ramachandran plot was further refined by editing the alignment (taking care that no gaps in the secondary structure region). The final refined model has 91.1% residues in the most favoured region and one residue in the disallowed region. The total quality G-factor was – 0.2, which is indicative of a good quality model (acceptable values of the G-factor in PROCHECK are between 0 and −0.5, with the best models displaying values close to zero). Based on verify 3D analysis, 85.89% of the residues had an averaged 3D-1D score > 0.2 which is indicative of a good model (Fig. 3B).

The structural superimposition of the model and the template using Align Structures program in DS, showed that the α-carbon coordinates differed by only 1.1 Å (Fig. 3B). Based on the topology diagram, the kinase domain of PknI consists of α-helix and β-strand, which is similar to those in alpha and beta (α + β) class of proteins. The ATP molecule was docked to the active site of PknI using Gold Software to study the interaction within the active site of PknI protein model. Based on Gold score and interaction between the protein and ligand, the best pose of ATP was selected. Both Lys 41 and Val 92 are found to interact with O1A and N1 atoms of ATP respectively (Fig. 3C).

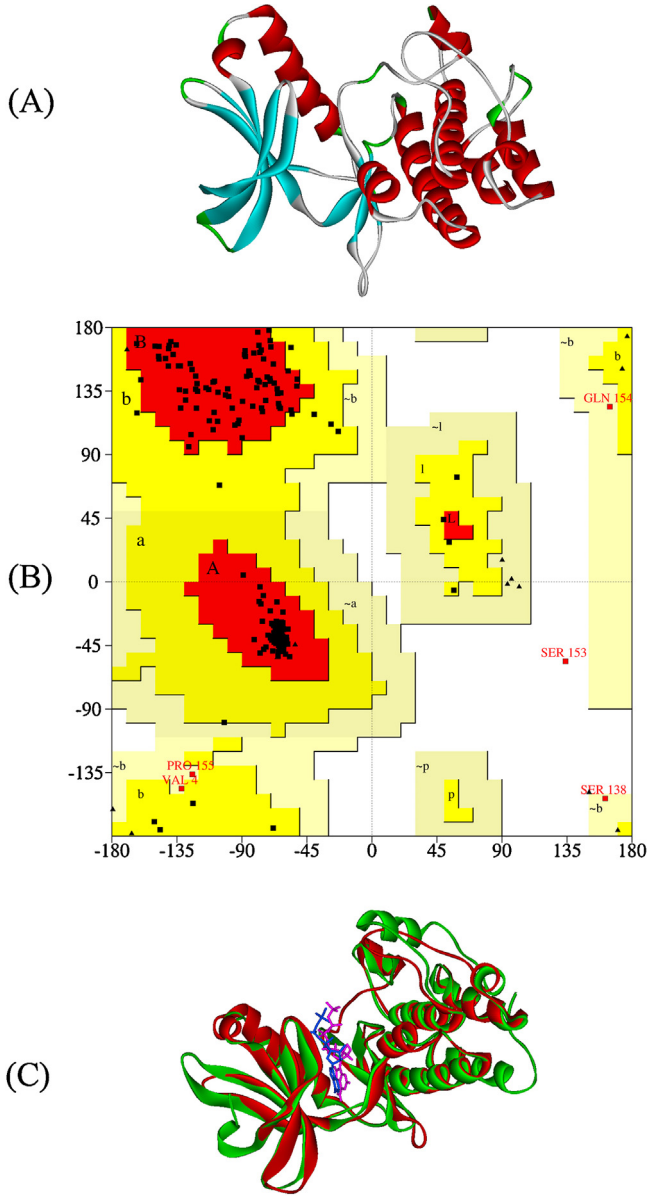

Fig. 3. 3D model of PknI, Ramachandran plot and PknI ATP complex image: (A) predicted structure for PknI. Helices, strands and turns are represented as red, cyan and green respectively. (B) Ramachandran plot of predicted structure of PknI protein estimated by PROCHECK. 91.1% residues of PknI protein fall in the most favoured region (red coloured). (C) The ATP molecule was docked into the active site of PknI using Gold Software and the best pose was revealed. The ATP was shown in violet and pink in colour. (For interpretation of the references to color in this figure legend, the reader is referred to the web version of this article.)

3.3. *Comparative structural analysis of PknI with other kinases*

Three dimensional structures of proteins are determined by their sequence and mutations in the sequences may or may not bring in any changes in their structures. Protein structures are more conserved than their sequences. The extent of high order

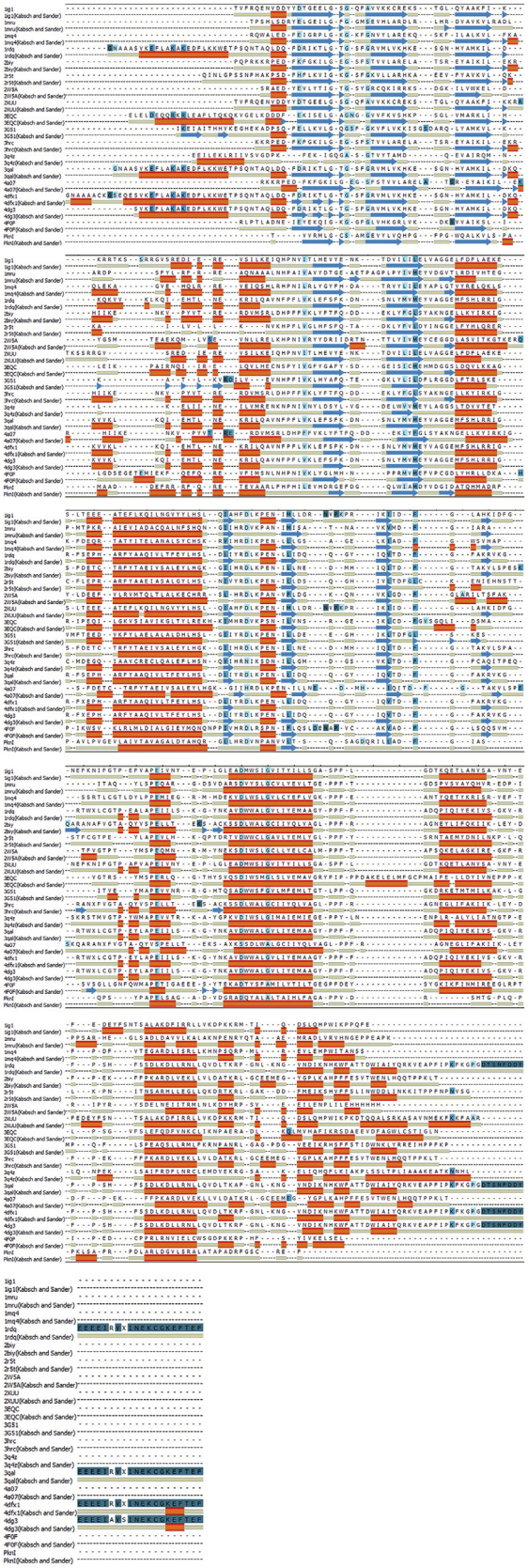

Fig. 4. Illustration of conserved secondary structure elements in protein kinases: The structural alignment contains eighteen protein kinases including the predicted PknI structure. Helices and strands are represented as red cylinders and blue arrows respectively. Identical and conserved residues are shaded in dark and light blue colour respectively. (For interpretation of the references to color in this figure legend, the reader is referred to the web version of this article.)

structural changes in response to sequence evolution will depend on the type and location of sequence changes. Some single mutations will completely disrupt structure, while others that conserve the physicochemical properties of the sequence will barely affect structure at all [45].

We have analyzed the secondary structure conservation between PknI and other kinase domain. The modelled structure of PknI was compared to Protein Data Bank (PDB) using SSM algorithm and 3D-PSSM fold recognition algorithm. The selected kinase proteins were superimposed using SSM and optimal structural alignment was obtained with high degree of conservity in the secondary structure elements with PknI (Fig. 4). The structural elements in the N-terminal regions are highly conserved than those in the C-terminal. Among the secondary structural elements, eight beta strands and eight alpha helices are highly conserved among these kinases. From the structural superimposition and alignment, it is observed that the cofactor binding site is highly conserved among the kinases. Furthermore, the structural alignment of PknI with other kinases clearly showed that the catalytic triad of each enzyme have a similar special position within the alpha and beta ($\alpha + \beta$) fold.

3.4. Structure based pharmacophore analysis of kinase structures bound with ATP

Totally, 21 co-crystal structures of kinase proteins from PDB were analyzed for better understanding of the interaction of the substrate and pharmacophore requirement in the active site of kinase proteins. In all the complexes, the three nitrogen atoms N1, N6 and N7 of adenosine are found to interact with the active site residues in different combinations. Of these, based on the consensus, N1 and N6 are found to interact with in all the selected structures. N1 atom and N6 atom of ATP were identified to interact preferentially with Valine and Glutamic acid residues respectively. The O2 and O3 atoms of the ribose moiety were identified interacting with Glu residue present within the active site. The O1A atom in the triphosphate moiety is identified to interact with Lys residues in all the protein structures analyzed. Based on the structure based pharmacophore analysis of ATP bound complexes, it is possible to get an in-depth view of their molecular recognition, which can be selected as the key residues that should interact with

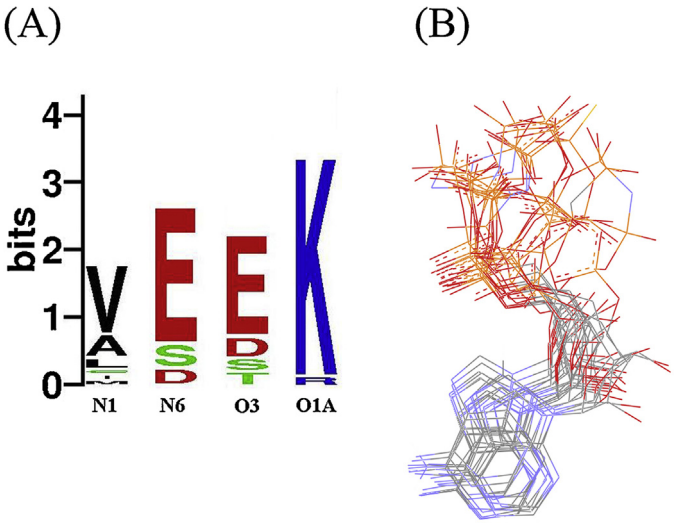

Fig. 5. PknI superimposition and active site mapping: (A) Sequence logo diagram for global consensus of active site residues interacting with N1, N6, O3 and O1A of ATP molecule based on pharmacophore analysis. (B) Structural superimposition of 17 bound ATP molecules from kinase complex structures.

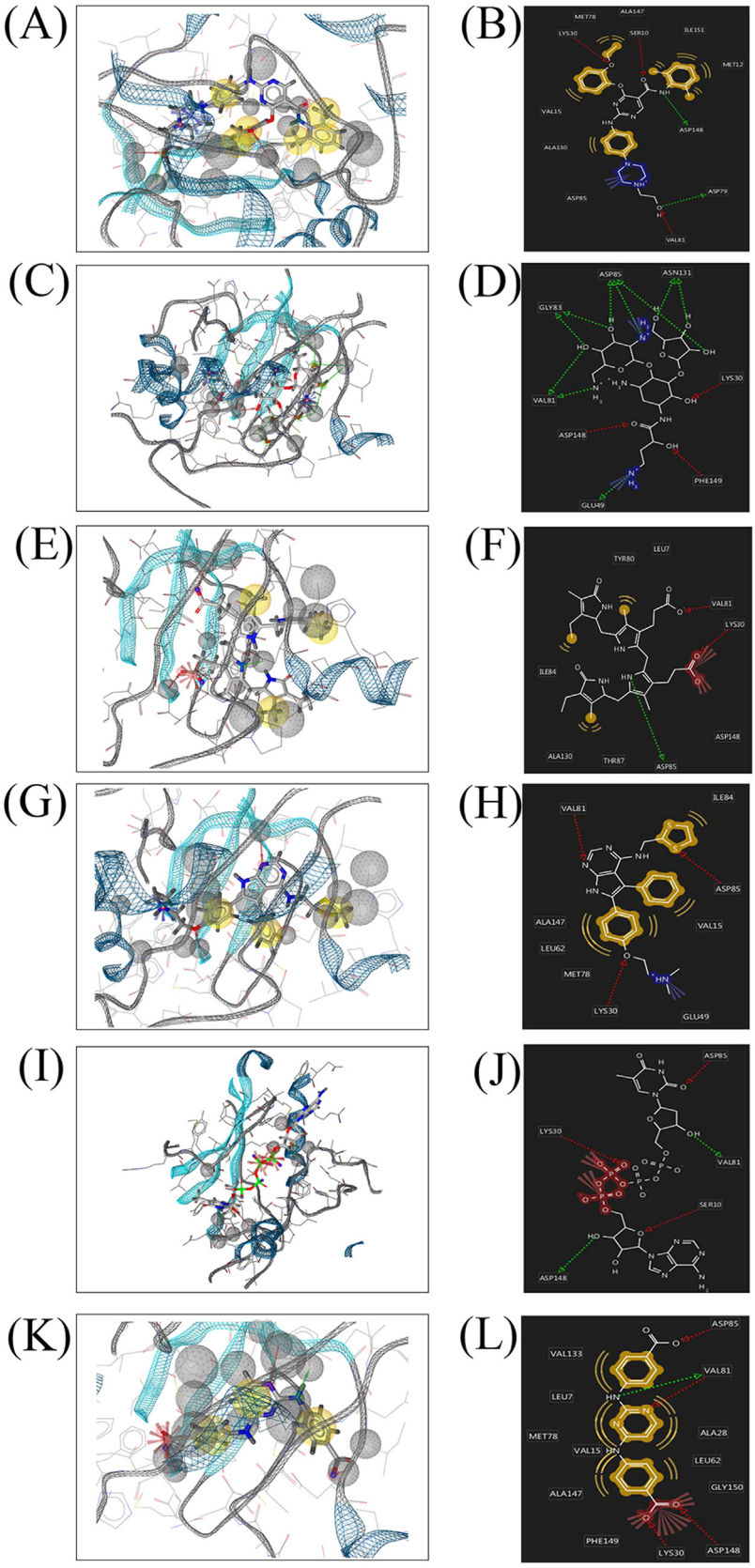

Fig. 6. PknI and six compound docking poses and interactions: The predicted docked poses of the best six drugs based on GOLD score in the pocket of PknI and its ligand interaction map was depicted in this image. The six drug interactions are shown in (A and B) (4TA), (C and D) (B31), (E and F) (BLA), (G and H) (NHI), (I and J) (T77) and (K and L) (T95). Green arrow represents the hydrogen bond donor (HBD); red arrow indicates hydrogen bond acceptor (HBA); yellow colour indicates hydrophobic (H); red shade indicates negative ionizable area and blue shade indicates positive ionizable area. (For interpretation of the references to color in this figure legend, the reader is referred to the web version of this article.)

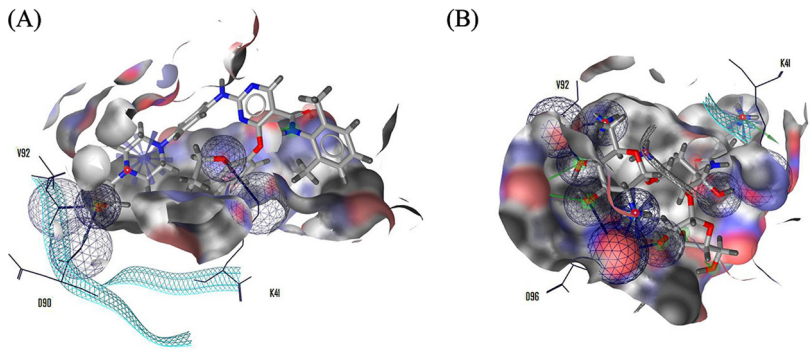

Fig. 7. PknI interaction with B31 and T95: (A) The 3D image depicts that B31 interaction with active site of PknI. (B) 3D view of T95 interaction with active site of PknI. Both the compound interacted with Lys 41 & Val 92 residues of PknI.

drug molecules. The consensus for the N1, N6, O3 and O1A are shown in (Fig. 5A). These residues were then mapped on to PknI structure to identify the critical residues such as Lys 41, Asp 96, Val 92, Asp 90. Superimposing the bound ATP molecules revealed that the adenosine and the ribose moiety are closely packed within the active site while the phosphate moiety is loosely packed with varying conformation (Fig. 5B). This additionally reveals the fact that the residues interacting with the adenosine and ribose moieties are the critical residues [42].

3.5. Molecular docking analysis

Molecular docking of drug molecules provides visualization of potential binding conformation and their hydrogen bonding interaction with the critical amino acid residues. A total of 2400 drug molecules in complex with kinase proteins were downloaded from Protein Databank and used for docking into the ATP site of PknI structure. For each of the molecules, 10 poses were produced and their corresponding gold fitness score were generated. Larger the fitness score better the ligand pose. A total of 152 molecules were selected as potent inhibitor based on the fitness score cutoff value of 70. These selected molecules were further validated by analyzing the binding mode of the selected drug molecules based on the interaction with the critical residues of PknI structure identified using structure based pharmacophore analysis. Totally, 6 hit molecules were selected as potent inhibitors based on the interaction with the critical residues (Fig. 6A–L and Table 2). Comparing the binding pose of all the 6 potent inhibitors of PknI, critical amino acids such as Lys 41 and Val 92 were identified to form hydrogen bond interaction with all the drugs and have good GOLD score (Table 2). Two compounds, T95 and B31, have the highest score 81.96 and 81.77 respectively. Analyzing their interaction with the active site residues of PknI structure, B31, like T95, forms interaction with Lys 41 and Val 92 but forms hydrogen bond with Asp 90 instead of Asp 96 (Fig. 7A). Whereas, T95 compound is found to form hydrogen bonding with the critical residues such as Lys 41, Asp 96 and Val 92 that also interact with adenosine and ribose moiety of ATP as discussed earlier (Fig. 7B). Kinase drugs are classified mostly into three types of pharmacophores type I, type II and type I1/2 [46]. Based on the pharmacophore features of the top 6 drugs identified, three drugs (T95, T77 and NHI) were classified as type II and I1/2 (Table 3). The pharmacophore of T95 almost resembled that of type II with two hydrophobic moieties and extend to the allosteric site. However, T77 and NHI are resembling type 1 1/2 group, bind the ATP site and extend to target the back cavity. Although, the remaining three drugs (B31, BLA and 4TA) form hydrogen bonds with the key residues in the active site of PknI, these drugs lacked a hydrophobic moiety. Thus, compounds B31 and T95 are predicted as potent inhibitors for PknI.

Table 2
List of functionally important residues of PknI.

Drug	Gold score	Functionally important residues			
		Lys 41	ASP 90	VAL 92	ASP 96
T95	81.96	+	–	+	+
B31	81.77	+	+	+	–
BLA	80.88	+	–	+	+
T77	75.05	+	–	+	+
4TA	72.59	+	–	+	+
NHI	71.91	+	–	+	+

Summary of best six drugs interactions score and critical amino acids essential for hydrogen bond formation. The Lys 42, Asp90, Val 92 and ASP 96 are critical amino acids of PknI which are involved in interactions with ligands. The '+' symbol indicates that the residue involved in the hydrogen bond formation and '–' symbol indicates that the residue was not involved in the hydrogen bond formation.

3.6. Site directed mutagenesis of lysine 41 to methionine in PknI protein

It was predicted that, the Lys 41 is very important for the functional activity of PknI protein. To confirm the functional importance of this residue, we mutated lysine 41 to methionine by using site directed mutagenesis. The mutated clone was confirmed by restriction enzyme digestion and the mutation was confirmed by sequencing analysis. The point mutant protein overexpression was confirmed by western blotting (Supplementary Fig. 2). Since, we already proved that PknI plays a role in cell division; the Ms-PknI over-expression strain (mc^2 4807) showed significant growth reduction when compared to control-Ms (mc^2 4806). But the point mutant strain (mc^2 4808) grew similar to that of control-Ms and further it did not reduce the growth when compared to mc^2 4807. These results indicated that, the Lys 41 residue was essential for PknI function (Fig. 8). Previously, we reported that the Lys41 point mutant of PknF in *M. smegmatis* mc^2 showed altered colony morphology, defective sliding motility and biofilm formation [11]. This study supports our present finding that Lys 41 residue was important for kinase activity. Similarly, two threonine residues in the PknB activation loop, namely Thr 171 and Thr 173 were identified as the target for PknB. Replacement of these threonine residues by

Table 3
Pharmacophore classifications of best six drugs.

Drug name	Pharmacophore classification
T95	Type II
B31	–
BLA	–
T77	Type 1 1/2
4TA	–
NHI	Type 1 1/2

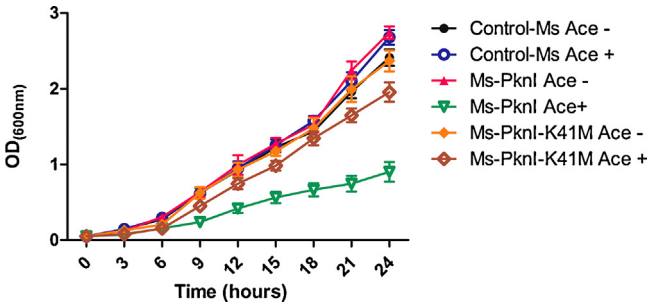

Fig. 8. *In vitro* growth kinetics of merodiploid strain: Strains harbouring acetamidase driven Ms-PknI, Ms-PknI-K41M and control-Ms were inoculated at a final OD_{600nm} of 0.05 into fresh medium and either induced with 0.2% acetamide or left uninduced. Aliquots of 1 ml were taken out from control uniduced ( ) and induced ( ), merodiploid strain harbouring Ms-PknI uninduced ( ) and induced ( ) as well as merodiploid strain harbouring Ms-PknI-K41M uninduced ( ) and induced ( ) every 3–24 h and measured for OD_{600nm}. Values are plotted are the averages and SD from triplicate experiments.

alanine significantly decreased the kinase activity [47]. In another study it was reported that, replacement of two conserved Threonine residues, namely Thr 171 and Thr 173 of PknJ did not show complete loss of activity as shown for PknB [48]. In our finding, the replacement of lysine 41 to methionine hampers the nucleotide binding site and thereby the kinase functions of PknI. Therefore, Lys 41 was predicted as an essential amino acid for PknI function.

Supplementary Fig. 2 related to this article can be found, in the online version, at http://dx.doi.org/10.1016/j.jmgm.2014.05.011.

4. Conclusion

In the present study, we have generated three dimensional structure of PknI and it has helped in understanding the conservative secondary structural pattern in kinase proteins. Comparative analysis of all PKNs in mycobacteria showed that highly conserved auto-phosphorylation threonine residue is totally absent in PknI. So the mode of substrate binding of PknI with substrates is questionable. Hydrogen bonding pattern between the docked and bound ATP molecules and active site residues of kinase proteins revealed lysine 41 of PknI as highly conserved and predicted to be catalytically important for kinase function. This was further proved by site directed mutagenesis of lysine 41 to methionine which hampers the binding of ATP to PknI.

Structure based pharmacophore analysis of kinase revealed that Lys41, Asp 90, Val 92 and Asp 96 residues are important for interactions with ATP. Based on docking score, 150 old drugs were selected. Using the structure based approach; we selected six drugs based on the interaction with critical amino acids. We further explored the binding mode of the six drugs with PknI structure. All the six drugs were identified to form hydrogen bond interactions with Lys41, Asp 90, Val 92 and Asp 96 amino acids. The two most potent drugs, T95 and B31 form additional hydrogen bond interactions. T95 forms additional hydrogen bond interaction with Ser 21; B31 forms hydrogen bonding with Phe 149, Gly94, Asn 142, Asp 159 and Glu 60. Based on docking score, both T95 and B31 drugs have the highest GOLD score, interacting with all the critical amino acids and are identified as potent inhibitors for PknI.

Acknowledgements

The authors wish to acknowledge Indian Council of Medical Research (ICMR) – Biomedical Informatics and National Institute for Research in Tuberculosis for the funding provided. Mr. Srinivasan Kandasamy received financial support from the Indian Council of Medical Research as Senior Research Fellow. We also thank Mr. Senthilnathan, National Institute for Research in Tuberculosis (NIRT) for editing figures.

References

[1] World Health Organization, Global Tuberculosis Control, 2012.
[2] S.H. Kaufmann, Envisioning future strategies for vaccination against tuberculosis, Nat. Rev. Immunol. 6 (2006) 699–704.
[3] J.B. Stock, A.J. Ninfa, A.M. Stock, Protein phosphorylation and regulation of adaptive responses in bacteria, Microbiol. Rev. 53 (1989) 450–490.
[4] Y. Av-Gay, M. Everett, The eukaryotic-like Ser/Thr protein kinases of *Mycobacterium tuberculosis*, Trends Microbiol. 8 (2000) 238–244.
[5] V. Molle, L. Kremer, Division and cell envelope regulation by Ser/Thr phosphorylation: Mycobacterium shows the way, Mol. Microbiol. 75 (2010) 1064–1077.
[6] C.M. Kang, D.W. Abbott, S.T. Park, C.C. Dascher, L.C. Cantley, R.N. Husson, The *Mycobacterium tuberculosis* serine/threonine kinases PknA and PknB: substrate identification and regulation of cell shape, Genes Dev. 19 (2005) 1692–1704.
[7] R. Chaba, M. Raje, P.K. Chakraborti, Evidence that a eukaryotic-type serine/threonine protein kinase from *Mycobacterium tuberculosis* regulates morphological changes associated with cell division, Eur. J. Biochem. 269 (2002) 1078–1085.
[8] A. Dasgupta, P. Datta, M. Kundu, J. Basu, The serine/threonine kinase PknB of *Mycobacterium tuberculosis* phosphorylates PBPA, a penicillin-binding protein required for cell division, Microbiology 152 (2006) 493–504.
[9] P. Deol, R. Vohra, A.K. Saini, A. Singh, H. Chandra, P. Chopra, T.K. Das, A.K. Tyagi, Y. Singh, Role of *Mycobacterium tuberculosis* Ser/Thr kinase PknF: implications in glucose transport and cell division, J. Bacteriol. 187 (2005) 3415–3420.
[10] A. Koul, A. Choidas, A.K. Tyagi, K. Drlica, Y. Singh, A. Ullrich, Serine/threonine protein kinases PknF and PknG of *Mycobacterium tuberculosis*: characterization and localization, Microbiology 147 (2001) 2307–2314.
[11] R. Gopalaswamy, S. Narayanan, W.R. Jacobs Jr., Y. Av-Gay, *Mycobacterium smegmatis* biofilm formation and sliding motility are affected by the serine/threonine protein kinase PknF, FEMS Microbiol. Lett. 278 (2008) 121–127.
[12] R. Gopalaswamy, S. Narayanan, B. Chen, W.R. Jacobs, Y. Av-Gay, The serine/threonine protein kinase PknI controls the growth of *Mycobacterium tuberculosis* upon infection, FEMS Microbiol. Lett. 295 (2009) 23–29.
[13] D. Kumar, K. Palaniyandi, V.K. Challu, P. Kumar, S. Narayanan, PknE, a serine/threonine protein kinase from *Mycobacterium tuberculosis* has a role in adaptive responses, Arch. Microbiol. 195 (2013) 75–80.
[14] A. Walburger, A. Koul, G. Ferrari, L. Nguyen, C. Prescianotto-Baschong, K. Huygen, B. Klebl, C. Thompson, G. Bacher, J. Pieters, Protein kinase G from pathogenic mycobacteria promotes survival within macrophages, Science 304 (2004) 1800–1804.
[15] K.G. Papavinasasundaram, B. Chan, J.H. Chung, M.J. Colston, E.O. Davis, Y. Av-Gay, Deletion of the *Mycobacterium tuberculosis* pknH gene confers a higher bacillary load during the chronic phase of infection in BALB/c mice, J. Bacteriol. 187 (2005) 5751–5760.
[16] V. Malhotra, L.T. Arteaga-Cortes, G. Clay, J.E. Clark-Curtiss, *Mycobacterium tuberculosis* protein kinase K confers survival advantage during early infection in mice and regulates growth in culture and during persistent infection: implications for immune modulation, Microbiology 156 (2010) 2829–2841.
[17] H. Lakshminarayan, A. Rajaram, S. Narayanan, Involvement of serine threonine protein kinase, PknL, from *Mycobacterium tuberculosis* H37Rv in starvation response of Mycobacteria, J. Microb. Biochem. Technol. 1 (2009) 030–036.
[18] A. Narayan, P. Sachdeva, K. Sharma, A.K. Saini, A.K. Tyagi, Y. Singh, Serine threonine protein kinases of mycobacterial genus: phylogeny to function, Physiol. Genomics 29 (2007) 66–75.
[19] A.E. Greenstein, C. Grundner, N. Echols, L.M. Gay, T.N. Lombana, C.A. Miecskowski, K.E. Pullen, P.Y. Sung, T. Alber, Structure/function studies of Ser/Thr and Tyr protein phosphorylation in *Mycobacterium tuberculosis*, J. Mol. Microbiol. Biotechnol. 9 (2005) 167–181.
[20] R. Gopalaswamy, P.R. Narayanan, S. Narayanan, Cloning, overexpression, and characterization of a serine/threonine protein kinase pknI from *Mycobacterium tuberculosis* H37Rv, Protein Expr. Purif. 36 (2004) 82–89.
[21] A. Singh, Y. Singh, R. Pine, L. Shi, R. Chandra, K. Drlica, Protein kinase I of *Mycobacterium tuberculosis*: cellular localization and expression during infection of macrophage-like cells, Tuberculosis (Edinb) 86 (2006) 28–33.
[22] S.K. Burley, An overview of structural genomics, Nat. Struct. Biol. 7 (2000) 932–934.
[23] J.M. Thornton, A.E. Todd, D. Milburn, N. Borkakoti, C.A. Orengo, From structure to function: approaches and limitations, Nat. Struct. Biol. 7 (2000) 991–994.
[24] J.D. Thompson, D.G. Higgins, T.J. Gibson, CLUSTAL W: improving the sensitivity of progressive multiple sequence alignment through sequence weighting, position-specific gap penalties and weight matrix choice, Nucleic Acids Res. 22 (1994) 4673–4680.
[25] S.F. Altschul, W. Gish, W. Miller, E.W. Myers, D.J. Lipman, Basic local alignment search tool, J. Mol. Biol. 215 (1990) 403–410.
[26] L.A. Kelley, M.J. Sternberg, Protein structure prediction on the Web: a case study using the Phyre server, Nat. Protoc. 4 (2009) 363–371.
[27] H.M. Berman, J. Westbrook, Z. Feng, G. Gilliland, T.N. Bhat, H. Weissig, I.N. Shindyalov, P.E. Bourne, The Protein Data Bank, Nucleic Acids Res. 28 (2000) 235–242.
[28] A. Fiser, A. Sali, Modeller: generation and refinement of homology-based protein structure models, Methods Enzymol. 374 (2003) 461–491.

[29] R.A. Laskowski, M.W. MacArthur, D.S. Moss, J.M. Thornton, PROCHECK: a program to check the stereochemical quality of protein structures, J. Appl. Crystallogr. 26 (1993) 283–291.
[30] R. Luthy, J.U. Bowie, D. Eisenberg, Assessment of protein models with three-dimensional profiles, Nature 356 (1992) 83–85.
[31] E. Krissinel, K. Henrick, Secondary-structure matching (SSM), a new tool for fast protein structure alignment in three dimensions, Acta Crystallogr. D: Biol. Crystallogr. 60 (2004) 2256–2268.
[32] G. Wolber, T. Langer, LigandScout: 3-D pharmacophores derived from protein-bound ligands and their use as virtual screening filters, J. Chem. Inf. Model. 45 (2005) 160–169.
[33] D. Joseph-McCarthy, B.E.t. Thomas, M. Belmarsh, D. Moustakas, J.C. Alvarez, Pharmacophore-based molecular docking to account for ligand flexibility, Proteins 51 (2003) 172–188.
[34] M.L. Barreca, L. De Luca, N. Iraci, A. Rao, S. Ferro, G. Maga, A. Chimirri, Structure-based pharmacophore identification of new chemical scaffolds as non-nucleoside reverse transcriptase inhibitors, J. Chem. Inf. Model. 47 (2007) 557–562.
[35] T.A. Young, B. Delagoutte, J.A. Endrizzi, A.M. Falick, T. Alber, Structure of *Mycobacterium tuberculosis* PknB supports a universal activation mechanism for Ser/Thr protein kinases, Nat. Struct. Biol. 10 (2003) 168–174.
[36] M.C. Good, A.E. Greenstein, T.A. Young, H.L. Ng, T. Alber, Sensor domain of the *Mycobacterium tuberculosis* receptor Ser/Thr protein kinase, PknD, forms a highly symmetric beta propeller, J. Mol. Biol. 339 (2004) 459–469.
[37] L.M. Gay, H.L. Ng, T. Alber, A conserved dimer and global conformational changes in the structure of apo-PknE Ser/Thr protein kinase from *Mycobacterium tuberculosis*, J. Mol. Biol. 360 (2006) 409–420.
[38] A. Cavazos, D.M. Prigozhin, T. Alber, Structure of the sensor domain of *Mycobacterium tuberculosis* PknH receptor kinase reveals a conserved binding cleft, J. Mol. Biol. 422 (2012) 488–494.
[39] N. Scherr, S. Honnappa, G. Kunz, P. Mueller, R. Jayachandran, F. Winkler, J. Pieters, M.O. Steinmetz, Structural basis for the specific inhibition of protein kinase G, a virulence factor of *Mycobacterium tuberculosis*, Proc. Natl. Acad. Sci. U. S. A. 104 (2007) 12151–12156.
[40] K.M. Briedis, A. Starr, P.E. Bourne, Analysis of the human kinome using methods including fold recognition reveals two novel kinases, PLoS ONE 3 (2008) e1597.
[41] N. Kannan, S.S. Taylor, Y. Zhai, J.C. Venter, G. Manning, Structural and functional diversity of the microbial kinome, PLoS Biol. 5 (2007) e17.
[42] M. Ortiz-Lombardia, F. Pompeo, B. Boitel, P.M. Alzari, Crystal structure of the catalytic domain of the PknB serine/threonine kinase from *Mycobacterium tuberculosis*, J. Biol. Chem. 278 (2003) 13094–13100.
[43] S.L. McGovern, B.K. Shoichet, Information decay in molecular docking screens against holo, apo, and modeled conformations of enzymes, J. Med. Chem. 46 (2003) 2895–2907.
[44] Z. Xiang, Advances in homology protein structure modeling, Curr. Protein Pept. Sci. 7 (2006) 217–227.
[45] K. Illergard, D.H. Ardell, A. Elofsson, Structure is three to ten times more conserved than sequence – a study of structural response in protein cores, Proteins 77 (2009) 499–508.
[46] F. Zuccotto, E. Ardini, E. Casale, M. Angiolini, Through the "gatekeeper door": exploiting the active kinase conformation, J. Med. Chem. 53 (7) (2010) 2681–2694.
[47] K.E. Lougheed, S.A. Osborne, B. Saxty, D. Whalley, T. Chapman, N. Bouloc, J. Chugh, T.J. Nott, D. Patel, V.L. Spivey, C.A. Kettleborough, J.S. Bryans, D.L. Taylor, S.J. Smerdon, R.S. Buxton, Effective inhibitors of the essential kinase PknB and their potential as anti-mycobacterial agents, Tuberculosis (Edinb) 91 (2011) 277–286.
[48] G. Arora, A. Sajid, M. Gupta, A. Bhaduri, P. Kumar, S. Basu-Modak, Y. Singh, Understanding the role of PknJ in *Mycobacterium tuberculosis*: biochemical characterization and identification of novel substrate pyruvate kinase A, PLoS ONE 5 (2010) e10772.
[49] S. Daugelat, J. Kowall, J. Mattow, D. Bumann, R. Winter, R. Hurwitz, S.H. Kaufmann, The RD1 proteins of *Mycobacterium tuberculosis*: expression in *Mycobacterium smegmatis* and biochemical characterization, Microbes Infect. 5 (2003) 1082–1095.
[50] C.K. Stover, V.F. De La Cruz, T.R. Fuerst, J.E. Burlein, L.A. Benson, L.T. Bennett, G.P. Bansal, J.F. Young, M.H. Lee, G.F. Hatfull, S.B. Snapper, R.G. Barletta, W.R. Jacobs, B.R. Bloom, New use of BCG for recombinant vaccines, Nature 351 (1991) 456–460.